Magnetic Resonance in Medicine 50:196–200 (2003)

Parallel Spectroscopic Imaging With Spin-Echo Trains

Ulrike Dydak, Klaas P. Pruessmann, Markus Weiger, Jeffrey Tsao, Dieter Meier, and Peter Boesiger*

A reduction in scan time in spectroscopic imaging (SI) can be achieved by both fast and reduced *k*-space sampling. This work presents an ultrafast SI technique that combines the two approaches. The synergy of multiple spin-echo (MSE) acquisition and sensitivity encoding (SENSE) enables high-resolution SI to be performed within a clinically acceptable scan time. MSE-SENSE-SI with echo train lengths ranging from one to four echoes is evaluated with respect to SNR and spatial response function by means of in vitro experiments. It is shown that acquiring two spin-echoes (SEs) per acquisition yields a good practical trade-off among scan time, SNR, and spatial response. The clinical feasibility of the technique is demonstrated in a patient with an astrocytoma, and SI data are obtained with an image matrix of 24 × 24 in just over 2 min. Magn Reson Med 50:196–200, 2003. © 2003 Wiley-Liss, Inc.

Key words: spectroscopic imaging; CSI; multiple spin-echoes; SENSE; parallel acquisition

Reducing the scan time in spectroscopic imaging (SI) while maintaining high spatial resolution is one of the challenges presented by the use of SI in clinical examinations. Considerable efforts have been directed toward developing methods to reduce the total duration of SI experiments. Such methods can be divided into two approaches: fast *k*-space sampling and reduced *k*-space sampling. SI sequences using fast *k*-space sampling are abundant. These methods range from *k*-space weighting by varying the repetition time (TR) (1), to multiple spin-echo (MSE) SI (2) and fast sequences based on various fast-imaging sequences, such as EPI, fast low-angle shot (FLASH), ultrafast low-angle RARE (U-FLARE), rapid acquisition with relaxation enhancement (RARE), gradient- and spin-echo (GRASE), and spiral imaging (3–9). All of these techniques offer a means of sampling at high speed the entire Fourier space, which is spanned by one spectral and two spatial dimensions. Frequently, this is done at the expense of parameter restrictions, such as reduced spectral resolution or bandwidth. MSE-SI exploits the fact that T_2 is much longer than T_2^* for the metabolites of interest, allowing the acquisition of several SEs for each excitation. By phase-encoding each echo separately, the speed of covering *k*-space can be enhanced by a factor that depends on the length of the spin-echo train (2). The latter is usually limited to the range of 2–4, reflecting the trade-off between spectral resolution, echo time (TE) requirements, and the need to avoid excessive T_2 decay.

The other approach to achieve faster SI is to reduce, rather than accelerate, the *k*-space sampling. The most typical way of doing so is to restrict *k*-space coverage to a circular region (2,10), which results in slightly reduced, radially isotropic resolution. Alternatively, or in addition, the number of *k*-space samples can be decreased by reducing their density. This is implicitly done, for instance, when a rectangular field of view (FOV) is fitted to the anatomy of interest (11). Further reduction of sampling density results in aliasing, and thus is not an option in conventional SI. However, with the advent of parallel MRI, this constraint has been significantly mitigated. Using arrays of receiver coils for signal detection, parallel techniques exploit the spatial encoding effect inherent to inhomogeneous coil sensitivity. This approach permits a reduction of the sampling density in *k*-space, for example, by a factor of 4, as recently demonstrated with sensitivity-encoded SI (SENSE-SI) (12,13).

In this work, we combined the benefits of reduced and fast *k*-space sampling by acquiring trains of MSEs in parallel SI. Unlike most other fast sampling schemes, MSE-SI performs phase encoding in both spatial dimensions, and thus favors sensitivity encoding with high acceleration factors (14). It is demonstrated that extremely short scan times of 2–3 min can be accomplished at relatively high spatial resolution by exploiting this synergy. However, with scan times in this range, one major concern is the signal-to-noise ratio (SNR), which inevitably decreases as the total acquisition is reduced. Therefore, the SNR behavior of the proposed approach was studied along with its general feasibility.

METHODS

SI experiments were carried out using conventional SI, MSE-SI, SENSE-SI, and MSE-SENSE-SI in a phantom and a patient with a grade II astrocytoma. The patient had undergone surgery and was being treated for reoccurring tumor by radiation therapy at the time of the measurement. Written informed consent was obtained prior to the study.

The experiments were performed at 1.5 T on Philips Gyroscan ACS NT and Philips Intera whole-body scanners, using a receiver array of six surface coils. Two coil elements were circular (diameter = 200 mm) and four were rectangular (100 × 200 mm). The array was arranged around the patient's head or the phantom as described in Ref. 13. The phantom was an ellipsoid filled with an aqueous creatine (CRE) solution (10 mmol/l concentration), containing three glass spheres (diameter = 40 mm). The glass spheres were filled with aqueous solutions containing only lactate (LAC) (left sphere, 10 mmol/l), LAC and N-acetylaspartate (NAA) (middle sphere, 5 mmol/l each), and only NAA (right sphere, 10 mmol/l) (Fig. 1a).

Institute for Biomedical Engineering, University of Zurich and Swiss Federal Institute of Technology Zurich, Zurich, Switzerland.

Grant sponsor: Swiss National Science Foundation; Grant number: 31-52173.97.

*Correspondence to: Prof. Dr. P. Boesiger, Institute of Biomedical Engineering, University and ETH Zurich, Gloriastrasse 35, CH-8092 Zurich, Switzerland. E-mail: boesiger@biomed.ee.ethz.ch

Received 12 August 2002; revised 6 February 2003; accepted 21 February 2003.

DOI 10.1002/mrm.10495
Published online in Wiley InterScience (www.interscience.wiley.com).

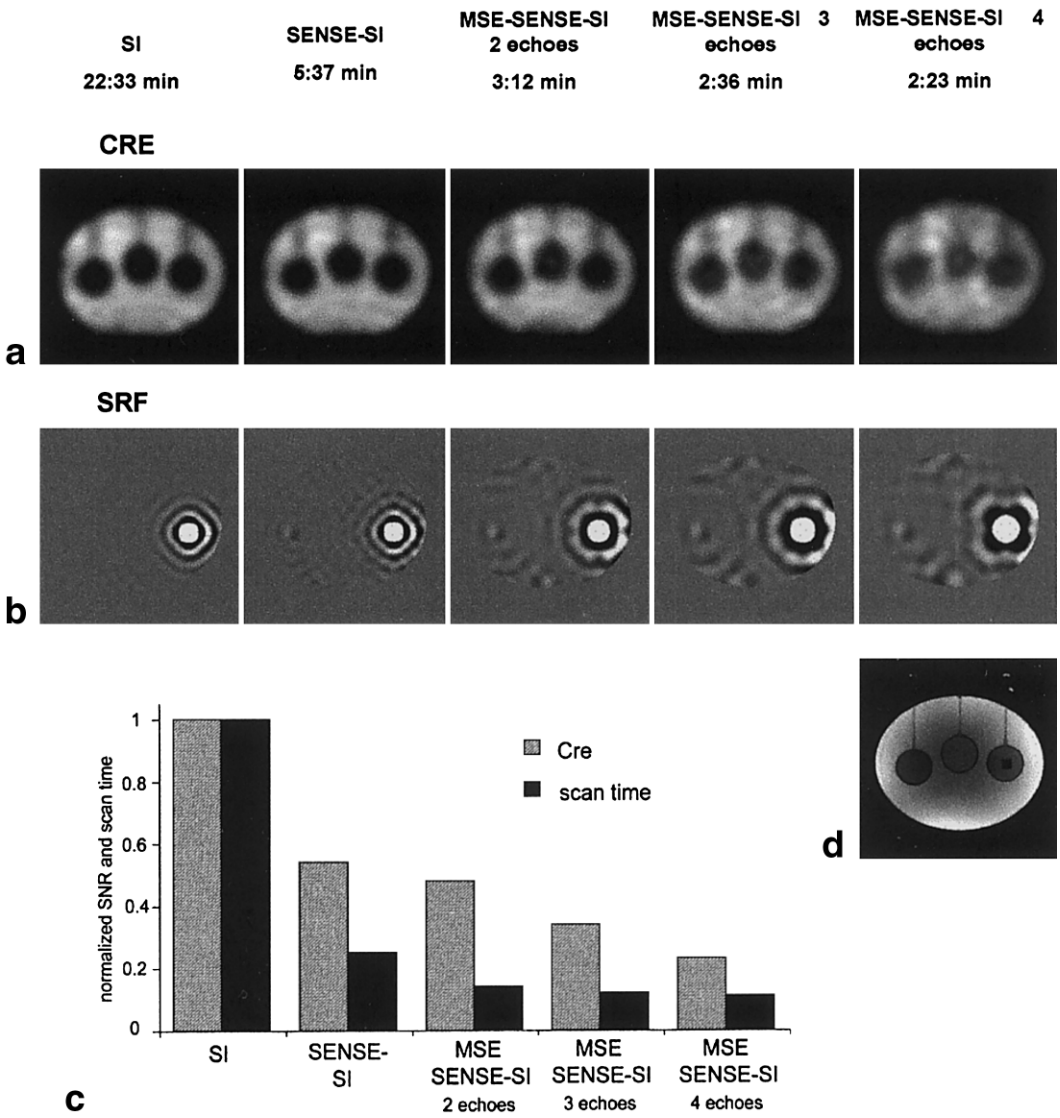

FIG. 1. In vitro SI measurements acquired with conventional SI, SENSE-SI, and MSE-SENSE-SI with SE trains ranging from two to four echos. **a:** CRE images, showing a decrease in SNR with reduced scan time. **b:** Real part of the spatial response function from the voxel outlined in the scout image. Additional blurring is visible in MSE-SENSE-SI acquisitions with longer echo trains. **c:** Mean SNR of CRE and scan time for the different acquisition schemes in the phantom study, normalized to an acquisition with conventional SI. **d:** Scout image of the phantom.

For high-resolution SI in vitro, a square field of view (FOV) of 230 mm, divided into 32 × 32 voxels, and a slice thickness of 15 mm were used, resulting in a nominal voxel volume of 0.77 ml. In vivo, a lower spatial resolution was chosen for shorter examination times. The nominal voxel size was 1.7 ml, using a square FOV of 220 mm, 24 × 24 voxels, and a slice thickness of 20 mm. In all cases, a circular *k*-space sampling scheme was applied (10). For SENSE, a reduction factor of 2 was chosen in both spatial dimensions, such that only every fourth point in spatial *k*-space was sampled. Using a repetition time (TR) of 1500 ms in vitro or 1700 ms in vivo, and a TE of 288 ms, 256 samples were acquired per spectrum over a bandwidth of 1000 Hz, yielding a spectral resolution of 4 Hz. Series of SI measurements were collected in vitro and in vivo, with and without using SENSE, keeping all parameters constant except for the echo train length. For the phantom measurement with an echo train length of 4, the TR had to be increased to 1700 ms to fit the acquisition of all echoes. Table 1 shows the scan times achieved with these settings, using conventional SI, SENSE-SI, and MSE-SENSE-SI with echo train lengths of two, three, and four echoes for both the in vitro and in vivo experiments. The scan time acceleration factors of the different techniques are not integer values, because of dummy scans and preparation phases that did not scale with the number of spin echoes or the number of *k*-space samples.

In all experiments, point-resolved spectroscopy (PRESS) volume selection (15) was combined with chemical shift-selective (CHESS) water suppression (16) and polygonal outer volume presaturation, as described in Ref. 2. Data were acquired simultaneously with all six receiver chan-

Table 1
Scan Times for Conventional SI, SENSE-SI, MSE-SI and MSE-SENSE-SI With Different Echo Train Lengths*

Resolution	Scantime (min:sec)								
	TR (ms)	SI	MSE SI	MSE SI	MSE SI	SENSE SI	MSE SENSE SI	MSE SENSE SI	MSE SENSE SI
Number of echoes	–	1	2	3	4	1	2	3	4
32 × 32 (in vitro)	1500	22:33	12:10	8:54	7:34	5:37	3:12	2:36	2:23 TR = 1700
24 × 24 (in vivo)	1700	14:02	7:54	5:59	4:38	3:37	2:13	1:55	1:33
Acceleration factor		1	~1.8	~2.4	~3	~4	~7	~8	~9

*For the in vitro study, a 32 × 32 matrix was acquired, using a TR of 1500 ms, whereas 24 × 24 voxels were acquired in the in vivo study, using a TR of 1700 ms. Acceleration factors indicate the ratio of total scan time and are averaged for both resolutions.

nels. Before Fourier transformation in all three dimensions, cosine filtering was applied in the spatial *k*-space dimensions. In the SENSE experiments, SENSE reconstruction was applied to the data, while sensitivity-weighted coil combination (17) was performed in the other cases. Further signal processing included Lorentz spectral filtering, a digital shift algorithm for improved water suppression (18), and constant baseline correction. Spectra were corrected for B_0 inhomogeneity based on a low-resolution reference scan without water suppression. The B_0 scan always preceded the actual measurement, and is included in the given scan times. Metabolic images of NAA, choline-containing compounds (CHO), CRE, and LAC were obtained by modulus integration of the respective peaks, and were Fourier-interpolated to 256 × 256 pixels.

The SNR of CRE in the in vitro spectra was calculated as follows: The signal strength of the CRE peak at 3.0 ppm was defined as the modulus signal amplitudes summed over a ±0.1 ppm interval around the peak center. The noise level was calculated as the standard deviation of the real part of the data in a peak-free area (9.42–7.13 ppm), normalized to the number of samples in the signal interval. To calculate a mean SNR, the SNR was averaged over several voxels within a region outside the glass spheres.

The spatial response function (SRF) for an SI voxel was calculated by taking into account the actual *k*-space sampling, the sensitivity weighting by the coil array, T_2 weighting of *k*-space in the case of multiple echoes (assuming a T_2 of 300 ms), and SENSE reconstruction in the case of the reduced-sampled data. This complex-valued SRF indicates the distribution of signal contributions to the reconstructed signal of the particular voxel.

RESULTS

In Vitro Experiments

Figure 1 shows the metabolite images of CRE (Fig. 1a) and the real part of the SRF (Fig. 1b) for the voxel marked in the scout image (Fig. 1d). The SI data were obtained in phantom measurements with conventional SI, SENSE-SI, and MSE-SENSE-SI with different echo train lengths ($N = 2, 3, 4$). No major residual aliasing artifacts were observed in the reconstructed SENSE data. However, the loss of signal with shorter scan time was evident. Blurring due to T_2 decay was visible in the CRE images of the MSE-SENSE-SI experiments, particularly with echo train lengths of three and four echoes, leading to reduced contrast. However, the main features of the phantom remained visible even at a ninefold scan time reduction.

Considering the trade-off between reduction in scan time and SNR, it did not seem worthwhile to use echo train lengths greater than two echoes. Figure 1c shows the in vitro scan times normalized to the scan time in conventional SI for SENSE-SI and MSE-SENSE-SI. In particular, the transition from three to four echoes per excitation hardly reduced the scan time (from 2.36 min to 2.23 min), because TR had to be increased to 1700 ms to fit four echoes. Figure 1c also shows the normalized mean SNR of CRE, as obtained in the phantom with the different acquisition schemes. While the acceleration in scan time approached a limit, the SNR dropped continuously with increasing echo train length. Considering minor scan time savings with long echo trains vs. increasing blurring and SNR loss, two SEs per TR were identified as the most effective choice in the given setup.

In Vivo Experiments

According to the in vitro results, the echo train length was set to two in an MSE-SENSE-SI study in a patient with a grade II astrocytoma. To permit comparison, conventional SI, SENSE-SI, MSE-SI, and MSE-SENSE-SI data were acquired from the same slice and with the same parameters. Metabolite images of NAA, CRE, CHO, and LAC are shown for all four acquisition methods in Fig. 2. Reduced NAA, as well as increased CHO and LAC in the right fronto-parietal region were readily detected with all techniques. However, scan time reduction clearly led to blurring and reduced SNR in the MSE-SENSE-SI images. The same observation was made in the spectra. Although all of the spectra from the voxel in tumorous tissue (Fig. 2e, voxel A in the anatomical image) clearly showed increased CHO, little NAA, and a large LAC peak, SNR loss was particularly obvious in this voxel. For other regions (as exemplified by voxel B in Fig. 2f), MSE-SENSE-SI yielded spectra of high quality, and there was a nearly sevenfold scan time reduction with respect to the conventional approach.

DISCUSSION

The current findings demonstrate that SENSE can be combined with MSE acquisition for fast SI. Using the hybrid technique, metabolite maps can be acquired substantially faster than with either of the two principles alone, and

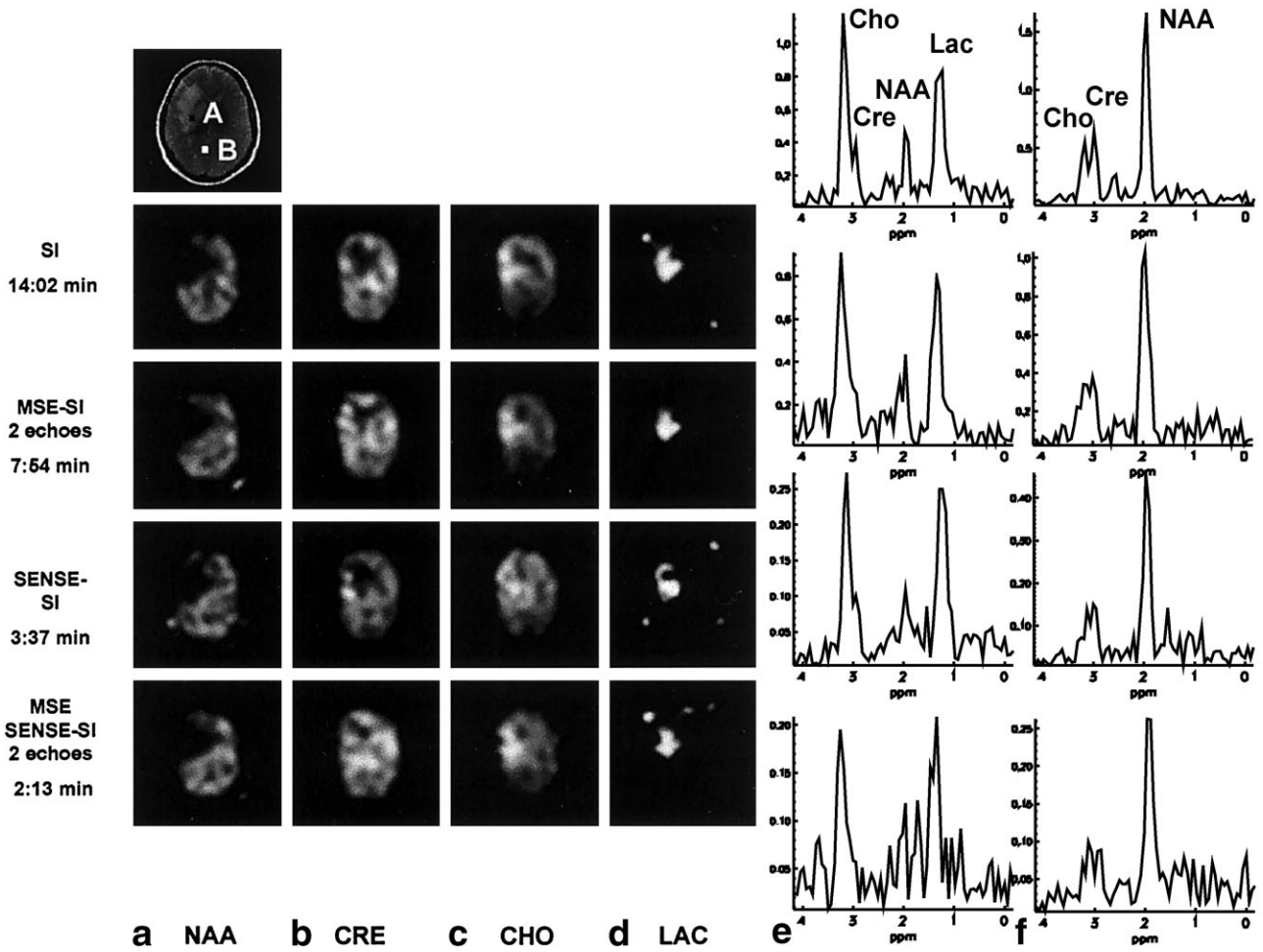

FIG. 2. Metabolite images of a patient with a grade II astrocytoma. (**a**) NAA, (**b**) CRE, (**c**) CHO, and (**d**) LAC images, as well as magnitude spectra from voxel A within (**e**) active tumor tissue and voxel B in (**f**) healthy tissue are shown for several acquisition techniques: conventional SI, double-SE SI, SENSE-SI, and double-SE SENSE-SI. The characteristic metabolic pattern of the astrocytoma is quite visible even with a ninefold scan time reduction using double-SE SENSE-SI.

seven to nine times faster than with conventional SI. High-resolution SI within approximately 2 min is thus made feasible, and the main characteristics of spectra and metabolite maps are preserved.

However, reducing the acquisition time in SI inevitably incurs a loss in SNR, which limits the potential of ultrafast techniques in general (19). In applications that require high SNR, sufficient signal averaging is indispensable, and reducing scan time may not be an option. In such situations, faster encoding may be used instead to cover larger brain areas in the same scan time. For instance, typical SI examinations may be extended to whole-brain coverage by resolving three spatial dimensions. For such purposes, parallel MSE acquisition is a promising option that should be further investigated.

Ultrafast SI is the method of choice when speed requirements outweigh SNR concerns. For instance, the proposed technique may be used for the acquisition of metabolic "scout images" with low resolution. Just as in common MRI, where fast, low-resolution survey images, which may also have low SNR, are acquired for the planning of high-quality images, an MSE-SENSE-SI scan of $\leq$3 min may be acquired (e.g., for the planning of a single-voxel study). In a fast scan, it is important to show the relevant structures in the metabolic images, while high SNR is less vital. Areas of large susceptibility differences, which should be avoided in the placement of a single voxel, would also be indicated by the MSE-SENSE-SI scan.

Higher field strength, which is becoming increasingly available in clinical environments, will significantly increase the potential of the presented technique. First, the gain of SNR at higher magnetic field strength is advantageous for MSE-SENSE-SI. Second, with increasing chemical shift, MSE-SI techniques can use shorter echo and acquisition times (20). In this fashion, T_2 decay is mitigated, and the SNR is enhanced considerably more than by higher field strength alone.

ACKNOWLEDGMENTS

The authors thank Philips Medical Systems, Best, The Netherlands, for their support in the implementation of the technique on the scanner.

REFERENCES

1. Kuhn B, Dreher W, Norris DG, Leibfritz D. Fast proton spectroscopic imaging employing k-space weighting achieved by variable repetition times. Magn Reson Med 1996;35:457–464.
2. Duyn JH, Moonen CTW. Fast proton spectroscopic imaging of human brain using multiple spin-echoes. Magn Reson Med 1993;30:409–414.
3. Posse S, Tedeschi G, Risinger R, Ogg R, LeBihan D. High speed 1H spectroscopic imaging in human brain by echo planar spatial-spectral encoding. Magn Reson Med 1995;33:34–40.
4. Haase A, Leibfritz D, Werk W. 31P FLASH NMR imaging. Magn Reson Med 1988;7:358–363.
5. Norris DG, Dreher W. Fast proton spectroscopic imaging using the sliced k-space method. Magn Reson Med 1993;30:641–645.
6. Dreher W, Leibfritz D. Improved proton spectroscopic U-FLARE imaging for the detection of coupled resonances in the rat brain in vivo. Magn Reson Imaging 1999;17:611–621.
7. Dreher W, Leibfritz D. Fast proton spectroscopic imaging with high signal-to-noise ratio: spectroscopic RARE. Magn Reson Med 2002;47:523–528.
8. Dreher W, Leibfritz D. A new method for fast proton spectroscopic imaging: spectroscopic GRASE. Magn Reson Med 2000;44:668–672.
9. Adalsteinsson E, Irarrazabal P, Topp S, Meyer C, Macovski A, Spielman DM. Volumetric spectroscopic imaging with spiral-based k-space trajectories. Magn Reson Med 1998;39:889–898.
10. Maudsley AA, Matson GB, Hugg JW, Weiner MW. Reduced phase encoding in spectroscopic imaging. Magn Reson Med 1994;31:645–651.
11. Golay X, Gillen J, van Zijl PC, Barker PB. Scan time reduction in proton magnetic resonance spectroscopic imaging of the human brain. Magn Reson Med 2002;47:384–387.
12. Pruessmann KP, Weiger M, Boesiger P. SENSE: sensitivity encoding for fast MRI. Magn Reson Med 1999;42:952–962.
13. Dydak U, Weiger M, Pruessmann KP, Meier D, Boesiger P. Sensitivity-encoded spectroscopic imaging. Magn Reson Med 2001;46:713–722.
14. Dydak U, Weiger M, Pruessmann KP, Meier D, Boesiger P. Sensitivity encoded multi-echo spectroscopic imaging. In: Proceedings of the 8th Annual Meeting of ISMRM, Denver, 2000. p 368.
15. Bottomley PA. Spatial localization in NMR spectroscopy in vivo. Ann N Y Acad Sci 1987;508:333–348.
16. Haase A, Frahm J, Haenicke W, Matthaei D. ^{1}H NMR chemical shift selective (CHESS) imaging. Phys Med Biol 1985;4:341–344.
17. Roemer PB, Edelstein WA, Hayes CE, Souza SP, Mueller OM. The NMR phased array. Magn Reson Med 1990;16:192–225.
18. Roth K, Kimber BJ, Feeney J. Data shift accumulation and alternate decay accumulation techniques for overcoming dynamic range problems. J Magn Reson 1980;41:302–309.
19. Pohmann R, von Kienlin M, Haase A. Theoretical evaluation and comparison of fast chemical shift imaging methods. J Magn Reson 1997; 129:145–160.
20. Lamerichs R, Harvey P, Folkers P, Meier D, Boesiger P. Fast spectroscopic imaging of human brain at 3 Tesla. In: Proceedings of the 9th Annual Meeting of ISMRM, Glasgow, Scotland, 2001. p 1693.